Steel and Composite Structures, *Vol. 29, No. 5 (2018) 681-688*
DOI: https://doi.org/10.12989/scs.2018.29.5.681

Influence of stiffener edge on the buckling load of holed composite plates

Mahnaz Zakeri *, Ali Mozaffari [a] and Mohamad A. Katirae [b]

Aerospace Engineering Department, K.N. Toosi University of Technology, Tehran, 16698-3911, Iran

(*Received June 2, 2018, Revised November 17, 2018, Accepted December 2, 2018*)

Abstract. In this paper, buckling load of edge stiffened composite plates is assessed. The effect of stiffener edge size, circular hole, and the fiber orientation angle on buckling behavior of composite plates under uni-axial compressive load is investigated. This paper includes two parts as experimental and numerical studies. L-shape composite plates are manufactured in three different layups. Then the buckling loads are experimentally determined. Subsequently, by using the numerical simulation, the size variation effects of stiffener edge and circular cutout on the plate buckling loads are analyzed in five different layups. The results show that cutout size, stiffener edge height and fiber orientation angle have important effects on buckling load. In addition, there is an optimum height for stiffener edge during different conditions.

Keywords: composite plate; buckling; finite element analysis; experiment; stiffener edge; cutout

1. Introduction

Currently, composite materials are widely used in majority of the modern engineering applications, in different shapes and styles, because of their high strength to weight, and stiffness to weight ratios and enhanced structural properties in comparison to common materials. In order to decrease weight and increase efficiency of airframe structures, one solution is to use these materials and awesome improvements are gained by doing so. Some aims such as decreasing weight, availability for monitoring, service access panels, passing hydraulic lines and cables, making windows, and doors force designers to make some cutouts in different sizes and shapes in a structure. Cutouts increase the structure's weight, except creating them to decrease weight (Niu 1988). While applying cutouts, it is necessary to reinforce the adjacent structures for supporting the applied load. Specially, structure's buckling load should be measured and represented for satisfying responses to ensure the structure's safety.

According to the type of structure and applied forces, the buckling load reaction is different, and it is classified. In some structures it is not allowed to buckle, but in others their post-buckling behavior are investigated. Generally, in thin-wall plates, buckling takes place before reaching the yield stress or failure load. As a result, the plates lose real resistance. Hence, buckling and post-buckling behavior analysis is extremely necessary. There are no comprehensive and precise methods for analyzing composite plates with cutouts. Some researchers have used the approximate methods, a large number have utilized the finite element methods, and only a few of them have done experimental researches on buckling and failure load of composite plates.

Martin's research (1972) was the first study on the buckling and post-buckling behavior of a rectangular composite plate with cutout under uni-axial compressive load. Larsson (1989) investigated the buckling behavior of linear elastic rectangular orthotropic plates with central circular cutout under uni-axial and biaxial compressive loads in clamp and simply supported boundary conditions by experimental and finite element methods. Nemeth (1988) studied the buckling behavior of symmetrically laminated angle-ply plates with centrally located circular hole by using FEM analysis and experimental method. In another research, he (1989) experimentally studied buckling and post-buckling behavior of isotropic and graphite-epoxy square plates with and without a central circular hole under uni-axial compressive load. Lin and Kuo (1989) numerically analyzed buckling of rectangular composite laminates with circular hole under in-plane compression loading; and investigated the effects of cutout size, ply lamination geometry and loading type. Hyre and Lee (1991) studied buckling performance of simply supported square plate with central hole, to show that buckling resistance can be improved by using the curvilinear fiber format. Britt (1993) investigated approximate analysis on shear and biaxial compressive buckling of anisotropic panels with a central elliptical cutout represented in two parts, pre-buckling and buckling. He also reported the effects of panel aspect ratio, cutout size and orientation, laminate anisotropy, and combined loading on the buckling load. Baily and Wood (1997) studied post-buckling behavior of square compression loaded graphite-epoxy panels by using FEM. These panels were under displacement loading with centrally and eccentrically square, elliptical and circular cutouts in clamped edge boundary conditions.

Jaunky (2001) addressed the progressive failure analysis results on flat and curved graphite-epoxy composite plates

*Corresponding author, Assistant Professor,
E-mail: m.zakeri@kntu.ac.ir
[a] Assistant Professor
[b] Ph.D. Student

ISSN: 1229-9367 (Print), 1598-6233 (Online)

with and without cutout under in-plane shear and compressive loading. Then he compared the results derived from finite element with experimental data. Jain and Kumar (2004) by a numerical method represented cutout size and shape effect (circular and elliptical) on buckling and first-ply failure loads of symmetric square laminates under uni-axial compression. Oterkus *et al*. (2004) studied the buckling of composite plates with a reinforced circular cutout under the uniform and non-uniform compressive load by the semi-analytical solution method. Eladi and Alecakir (2006) experimentally searched for failure loads of the stiffened carbon-epoxy panels with and without cutout under compression loads (manufactured by the resin transfer molding). Ghannadpour *et al*. (2006) represented the elliptical and circular cutouts effect on buckling behavior of rectangular polymer matrix composite plates, by using the finite element method. They also investigated the effect of cutout size on plates with different aspect ratio for symmetric cross-ply laminate. Yazici (2008) studied the effects of cutout size, orientation and corner radius on buckling behavior of polymer matrix composite plates considering simply supported boundary conditions on loaded edges and free boundary conditions for unloaded edges by finite element method.

Moen and Schafer (2009) developed closed-form expressions in order to estimate effect of single or multiple cutouts on critical elastic buckling stress of plates in bending or compression. Tercan and Aktaş (2009) performed the buckling behavior of 1×1 rib knitting glass-epoxy laminated plates with cutouts (circular, elliptical, square, and rectangular) and without cutouts by finite element and experimental methods. Kumar and Singh (2010, 2011) reported the effects of flexural boundary conditions, cutout geometry and shear loading orientation on buckling and post-buckling responses of composite laminates by using numerical analysis. Also, they addressed the interaction curves along with buckling and post-buckling responses. The samples were quasi-isotropic and orthotropic laminates under uni-axial compression combined with in-plane shear loads. Lopatin and Morozov (2013) analyzed the buckling of uniformly compressed rectangular composite sandwich plates based on Lagrange principle and first-order shear deformation theory. The boundary conditions considered two parallel edges simply supported, one edge clamped and the remaining edge free. They used the Kantorovich procedure and the generalized Galerkin method to recognize an analytical formula for critical loads verified by using finite element analysis.

Talib *et al*. (2013) studied the influence of cutout on multi-layer Kevlar-29/epoxy composite laminated plates under quasi-static compressive and tensile load by experimental method. Finally, they compared the experimental results with finite element analysis and showed that the test results have a good matching with numerical ones. Upadhyay and Shukla (2013) investigated post-buckling behavior of composite skew plates under in-plane uni-axial compressive and shear loadings considering higher order shear deformation theory. Umut (2013) utilized a new extended layerwise optimization method for maximization of the critical thermal buckling load of laminated composite plates as the design objective and the fiber orientations as design variables. Abolghasemi *et al*. (2014) searched for buckling of functionally graded plates with an elliptical cutout under combined thermal and mechanical loads using FEM. They studied the effect of boundary conditions, plate aspect ratios and cutout radius ratios on thermo-mechanical buckling behavior of the plates. Aktaş and Balcıoğlu (2014) studied the effects of plate thickness, the diameter of circular cutouts, the distance between circular cutouts, and rowing orientation angles on the buckling load of pultruded composite beams with single and double circular cutouts. Chen and Qiao (2014) analyzed the post-buckling of laminated plates under combined shear and compression using the nonlinear finite strip method.

Bohlooly and Mirzavand (2015) represented closed form solutions for buckling and postbuckling behavior of symmetric laminated composite plates with surface mounted and embedded piezoelectric actuators subjected to mechanical, thermal, electrical, and combined loads. Subsequently, they presented (Bohlooly and Mirzavand 2016) a thermo-mechanical buckling analysis for cross-ply laminated composite plates integrated with piezoelectric actuators, by utilizing the classical laminated plate theory and the von-Karman non-linear kinematic equations.

Jamali *et al*. (2016) assessed buckling of the nanocomposite plate with a central square cutout reinforced by carbon nanotubes surrounded by Pasternak foundation. Biswal *et al*. (2016) studied the effects of moisture and temperature on buckling behavior of laminated composite cylindrical panels by numerical and experimental methods. Also they considered effects of curvature, lamination sequences, number of layers and aspect ratio on buckling of composite curved panels subjected to hygrothermal load.

Sun *et al*. (2017) addressed cutout effects on stress concentrations, failure styles, natural frequencies and mode shapes of carbon fiber reinforced lattice-core sandwich cylinder by experimental and numerical methods. Lu *et al*. (2017) based on an energy method studied buckling response in electrospun fiber with periodic structure. They conducted an approximate mechanical approach for the critical load and the number of half waves in the buckled shape. Narayana *et al*. (2018) studied effects of volume fraction, fiber and resin type, and size of square/rectangular cutout on thermal buckling behavior of symmetrically laminated composite plates by using finite element method. In another research, Wang *et al*. (2018) investigated the torsional buckling of grapheme platelets reinforced functionally graded cylindrical shell with cutout using finite element method.

In summary, the buckling of laminated plates has been widely investigated to find the effect of various parameters like; cutout size and shape, fiber orientation angle, place and type of applied load. However, there is limited information about combination of these factors and stiffened composite plates need more investigation. This paper is divided in two parts: one experimental and the other one numerical. In this study, some experiments are accomplished on E-glass/epoxy L-shaped specimens with and without circular cutouts under uni-axial compressive load, and the buckling loads are measured. In addition, the

material properties of manufactured samples are determined by using standard coupon tests. Then, the effect of stiffening edge' height and circular cutout size on buckling loads of the composite plates are investigated by FEM in five different layups (with the same properties of experimental samples).

2. Experimental study

In this part, effects of layup, existence and nonexistence of circular cutouts on the buckling behavior of E-glass/epoxy L-shaped samples, which are prepared by the hand layup method, are experimentally investigated.

2.1 Geometry and layup of samples

The geometry of experimented specimens and their dimensions are presented in Fig. 1 and Table 1 respectively.

In these samples, three different layups of [0/0/0], [0/45/0] and [45/-45/45] are investigated. In each configuration, three samples including the hole and three other ones without hole are prepared. During making the specimens, no additional reinforcement has been used in the thickness direction (such as stitching, *z*-piping, etc.).

2.2 Specimens' material and production method

The Materials used to prepare L-shape samples are Glass fibers and Epoxy resin. The fibers are in the form of uni-directional E-glass fabric from Metyx with 621 gr/m^2 weight. The resin is LY5052 type epoxy, and the hardener is HY5052 type. The mix ratio of the resin with the hardener is 100 gr to 38 gr, respectively. Moreover, 4 gr of Aerosil powder is added. Finally, after mixing and making the mixture slick, it is used to layup the fibers by the hand layup method.

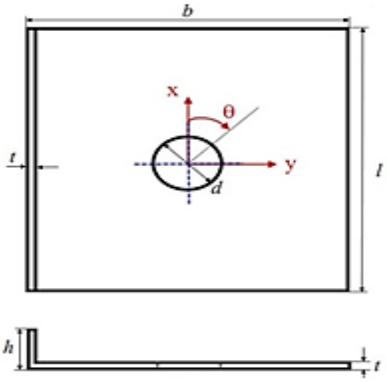

Fig. 1 Samples geometry

Table 1 Dimensions of specimens

Symbol	(mm)
l (plate length)	100
b (plate width included the stiffener)	100
h (the stiffener height including the plate thickness)	20
t (thickness of plate and stiffener)	2

Regarding the production method and samples geometry, it is necessary to make a special mold. The mold is made up of low carbon steel of type ST-37. It has two pieces (hermaphrodite), each of which fastens the other one by four screws. In the female mold, three openings are designed to remove extra resin after the screws were fastened on the mold. In addition, there are some step edges in the mold to make L-shaped sample. Direction of the fibers is laid-up according to x-axis shown in Fig. 1, and the mold is fastened. Then, each sample is kept in ambient temperature (about 27 centigrade) for 20 hours to dry completely. After leaving the mold, the samples are cut to specific size by the air body saw.

Half of the samples include a central circular cutout with 20 mm diameter. The hole is made by drilling milling machine with the four head end mill in type of HSS-Q20. The drilling milling machine is Lunan that consists of a precise digital ruler. Also it simultaneously cuts the surface and side, and makes a slick hole, and prevents delamination. Drilling is done by low discontinuous compression with 220-rpm speed. For creating more precise cutouts, a polyamide jig is designed. Finally, 18 L-shaped specimens are manufactured. For simulation and FE analysis of each specimen, it is necessary to know the material properties. For this purpose, by using the same materials of specimens, some coupons are manufactured and tested in different layups and sizes according to the D3039 (2000) and D3518 (1995) of ASTM standards. For each standard model, three coupons are made, so there are nine coupons, at last. The specimens and coupons are put in an oven with the closed door in order to cure them. The oven primary temperature is the same as ambient temperature that is 26℃. Then the temperature increases 4℃ per 15 min to reach 50℃. Afterwards, they are kept for 15 hours in this temperature. Finally, the oven temperature decreases 4℃ per 15 min to get to the ambient temperature, again.

2.3 Boundary and test conditions

In order to test the specimens, it is necessary to design and create a suitable fixture for applying uni-axial compressive load on the specimens. For this purpose, a low carbon steel fixture of type ST-37 is prepared. In each fixture's part, there is a circle plate with 8 mm thickness. These plates are cut by wire cut device (Agie-cut 200), according to the specimens' sizes and shapes which are 8 mm in depth and 2 mm in width. During the test, the center of each specimen is aligned with the center of fixture. In addition, applied load completely passes through the center of fixture. For testing, both up and down edges of L-shaped specimens are pressed fit on the grooves at a depth of 8 mm, which are carved into the fixture.

In addition, Instron-5500R is the device used for test that has two fundamental features that are parallel jaws and precise load cell. The fixture and L-shaped specimen are vertically and straightly set on the test part of machine. Each specimen is put under the uni-axial compressive load according to ASTM-D6641 (2001) with rate of 1.3 mm/min by displacement loading. It continues until ultimate failure

Fig. 2 Fixture parts with a testing sample

of each part occurs. Fig. 2 shows the designed fixture and one buckled specimen. It should be noted that the axial displacement and load outputs are collected by a data-acquisition system, and a computer records them.

2.4 Experiment

2.4.1 Material characterization

The average amounts of material properties obtained from test results of standard coupons are shown in Table 2. Resin and fibers weight percentage in the specimens are measured by elimination method of resin from fibers. In order to perform finite element analysis on the samples using Ansys software, G_{13}, G_{23}, and υ_{23} parameters are needed in addition to mentioned data in Table 2. Hence, by referring to previously published results by Tercan and Aktaş (2009) and composite material handbook (2002) these parameters are approximately assumed as G_{23} = 0.6×G_{13} = 2.31 GPa, and υ_{23} = 0.45.

Table 2 Material properties

Symbol	Unit	
E_{11}	(GPa)	22.47
E_{22}	(GPa)	6.28
E_{33}	(GPa)	6.28
G_{12}	(GPa)	3.5
G_{13}	(GPa)	3.5
υ_{12}	_	0.275
υ_{13}	_	0.275
ρ	(kg/m^3)	1800
w_f	_	61.53
w_m	_	38.47

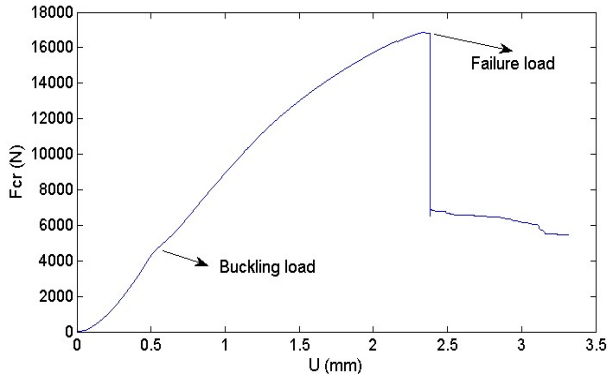

Fig. 3 Load–displacement diagram of S11 sample

2.4.2 Experimental results

In order to determine the buckling loads, the axial load versus the axial displacement diagram (Fig. 3) is used for each specimen. The first point of slope change in most of these diagrams occurs on the primary buckling point. Because of a large number of date points around the bifurcation point (critical buckling load), it is possible to recognize this buckling point easier by numerical data limitation for drawing diagram; although their extraction were not possible in four cases.

Finally, the results derived from test are presented in Tables 3-4. In these tables, $F_{ex.}$ is experimental buckling load of specimens. It is mentioned that all specimens have buckled before reaching the failure point. The failure of specimens with [0/0/0] and [0/45/0] layups occurred with loud sound and a sudden downfall of load, but in the specimens with [+45/-45/+45] layup it occurred with low sound and slow load reduction. Fig. 4 shows buckle to failure stages for one of the specimens.

The results presented in Tables 3-4 show that buckling in the holed samples occurs on lower load in comparison with the samples without cutout. Also, the specimens with [0/0/0] layup have the highest buckling load.

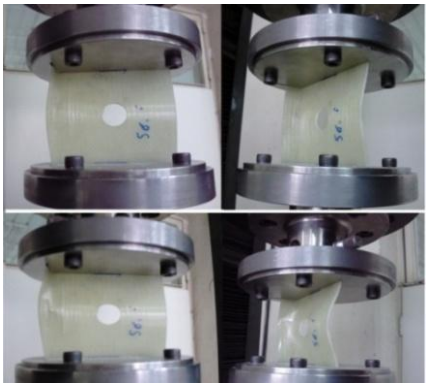

Fig. 4 Buckling to failure stages of S6 sample

Table 3 The samples test results without cutout

Lay-up	Sample	$F_{ex.}$ (Buckling load) (N)	Average of buckling loads (N)
[0/0/0]	S1	*	6900
	S2	7000	
	S3	6800	
[0/45/0]	S7	6500	6350
	S8	*	
	S9	6200	
[+45/-45/+45]	S13	2950	3100
	S14	*	
	S15	3250	

* The impossibility of accurate detecting the slope change point

Table 4 The samples test results with cutout

Lay-up	Sample	$F_{ex.}$ (Buckling load) (N)	Average of buckling loads (N)
[0/0/0]	S4	5800	5900
	S5	*	
	S6	6000	
[0/45/0]	S10	4500	4316
	S11	4250	
	S12	4200	
[+45/-45/+45]	S16	2100	2223
	S17	2070	
	S18	2500	

* The impossibility of accurate detecting the slope change point

Table 5 Comparison of the experimental and numerical buckling loads

Lay-up	d (mm)	EXP. (N)	Ansys (N)	Error (%)
[0/0/0]	0	6900	6989	1.2
	20	5900	6038	2.3
[0/45/0]	0	6350	6542	3.1
	20	4316	4415	2.2
[+45/-45/+45]	0	3100	3215	3.7
	20	2223	2292	3.1

Table 6 Variable parameters values for FEM models

h (mm)	0	4	7	12	20	25	30	40	50
Lay-up	[0/0/0],	[0/90/0],	[0/45/0],	[+45/0/-45],	[+45/-45/+45]				
d (mm)	0	5	10	20	30	40	50	60	

3. Finite element analysis

In this section, at first, the experimented samples in previous section are modeled to get the numerical buckling load by using Ansys 10. In Table 5, finite element results are compared with the experimental date. As it is seen, the results are in close agreement with each other.

Then in five different layups, various models are created with different stiffener height and circular cutout size (Table 6). Afterward the buckling analysis is done. The models have the same material properties and boundary conditions as tested samples. They are meshed using quadrilateral elements (SHELL 91). This element has six degrees of freedom at each node, translations in the nodal *x*, *y*, and *z* directions and rotations about the nodal *x*, *y*, and *z*-axes (Desalvo 1983). After performing a mesh convergence study, each model has about 4200 elements and 13000 nodes.

For creating the boundary conditions, all nodes on the lower edge with 8 mm width are clamped the same as tested samples. However, all nodes on the upper edge with the same width are constrained so that the axial displacement is possible just along the applied load, and other degrees of freedom are closed completely.

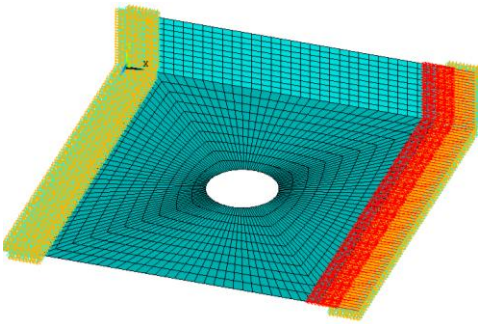

Fig. 5 A finite element model of the holed plate

In order to achieve the buckling loads by Ansys software, a unit load can be applied on the plate edges before solving in modal mode. Then, the obtained frequency is equal to the buckling load. In our analysis, the loading is the unit uni-axial compressive load that is uniformly distributed across the upper edge nodes. Fig. 5 shows an example of finite element models.

3.1 Discussion on the results

The diagrams of the non-dimensional buckling load on cutout size and non-dimensional buckling load on stiffener edge size are illustrated in Figs. 6(a)-(i) and Figs. 7(a)-(h). In these figures, N_x is the numerical buckling load (F_{cr}) per unit width (F_{cr}/b). As it is seen in Fig. 6, increasing of cutout size leads to decrease in buckling load generally, although the existence of small cutouts ($d/b \leq 0.05$) in some cases leads to the buckling load improvement. It seems that these cutout types work as a constraint.

Between the used layups, fibers with orientation 0° with respect to major axis (*x*-axis) increase the buckling load more than other fiber orientation angles. In addition, it is seen in Figs. 7(a)-(h) that for a plate with or without cutout increasing the stiffener edge size leads to the buckling load improvement in models primarily, but the buckling load becomes stable and constant, finally. It shows that the larger size of edge in comparison to the optimum size of stiffener edge catches the premature buckling. Thus, it does not have a remarkable effect on increasing the buckling load. It should be noted that the optimum size of stiffener edge is affected by cutout size and it changes in different layups.

4. Conclusions

In this paper, a finite element model has been used to find the buckling load of edge stiffened composite plates with a central hole. Experimental tests were also carried out to confirm the numerical results. There was a good agreement between the numerical and experimental results.

The most important results of this study are:

- The experimental results show that the specimens with cutout have lower buckling load in comparison to the specimens without cutout.

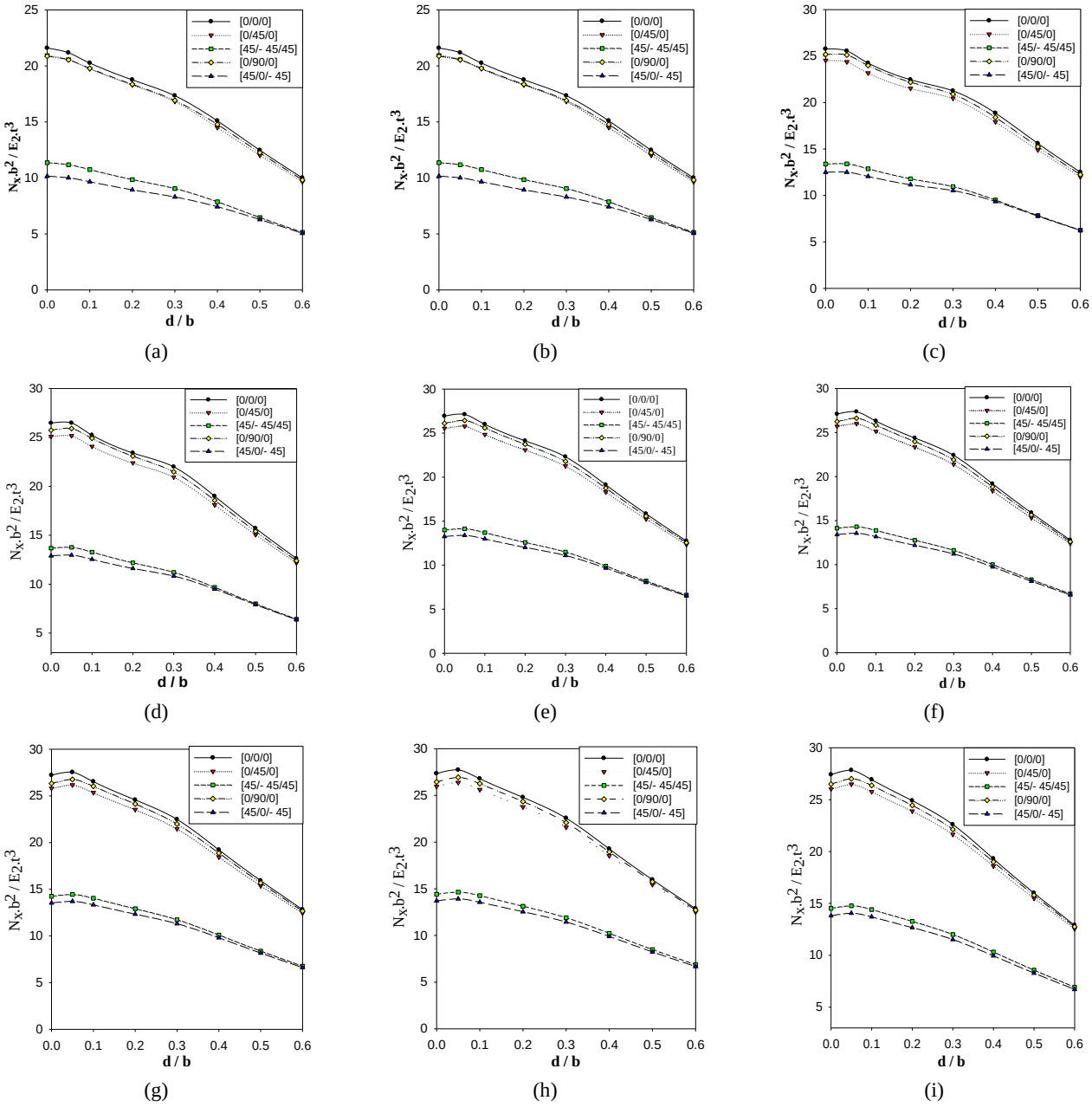

Fig. 6 Variations of non-dimension buckling loads on cutout size in different stiffener edge height: (a) h/b = 0; (b) h/b = 0.04; (c) h/b = 0.07; (d) h/b = 0.12; (e) h/b = 0.2; (f) h/b = 0.25; (g) h/b = 0.3; (h) h/b = 0.4; and (i) h/b = 0.5

- In the tested samples with and without hole, the highest buckling load is related to the specimens with [0/0/0] layup.
- [+45/-45/+45] layup has saliently the least amount of buckling load among the specimens. It shows that increasing the percentage of using 45-degree fibers is not always useful.
- The results of finite element analysis show that the cutout size affects the buckling load. In these models, by changing the size of (d/b) from zero to 0.6, the buckling load decreases to 50%. However, small cutouts of (d/b) < 0.05 do not greatly affect the bucking load, and even sometimes, there is a positive effect that totally is ignorable.
- In the plates with the constant stiffener edge size, buckling load decreases by increasing the hole diameter. However, in the constant size cutout, by increasing the stiffener edge size, buckling load increases at the beginning, but finally it becomes stable and constant. It means that there is a suitable optimum height for stiffener edge in different conditions. In this way, by increasing the edge height, only more materials are used that result in an overweight structure; however it does not have a considerable effect on buckling load. Also, for the models with (d/b) = 0.2, the best (h/b) for the stiffener is 0.25.
- Moreover, investigation on the ratio of buckling load for stiffened plate to plate without edge with the same cutout size shows that applying the best height

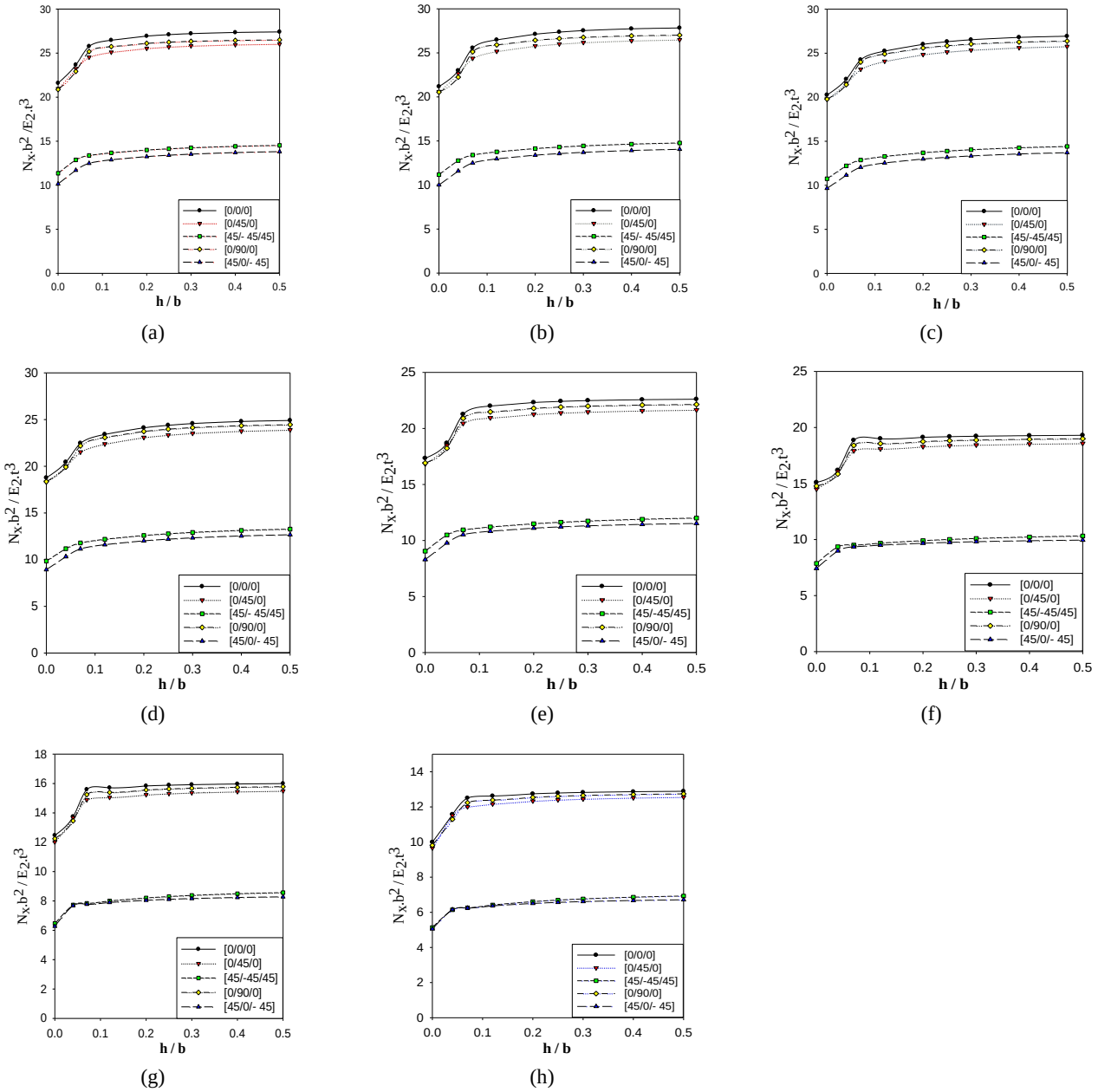

Fig. 7 Variations of non-dimension buckling loads on stiffener edge height in different cutout size: (a) d/b = 0; (b) d/b = 0.05; (c) d/b = 0.1; (d) d/b = 0.2; (e) d/b = 0.3; (f) d/b = 0.4; (g) d/b = 0.5; (h) d/b = 0.6.

can improve the buckling load up to 30 percent.

References

Abolghasemi, S., Shaterzadeh, A.R. and Rezaei, R. (2014), "Thermo-mechanical buckling analysis of functionally graded plates with an elliptic cutout", *Aerosp. Sci. Technol.*, **39**(1), 250-259.

Aktaş, M. and Balcıoğlu, H. (2014), "Buckling behavior of pultruded composite beams with circular cutouts", *Steel Compos. Struct., Int. J.*, **17**(4), 359-370.

American Society for Testing and Materials (1995), Standard test method for in-plane shear response of polymer matrix composite materials by tensile test of a ±45° laminate-Designation D3518; ASTM International, West Conshohocken, PA, USA.

American Society for Testing and Materials (2000), Standard test method for tensile properties of polymer matrix composite materials-Designation D3039; ASTM International, West Conshohocken, PA, USA.

American Society for Testing and Materials (2001), Standard test method for determining the compressive properties of polymer matrix composite laminates using a combined loading compression (CLC) test Fixture-Designation D6641; ASTM International, West Conshohocken, PA, USA.

Baily, R. and Wood, J. (1997), "Post buckling behavior of square compression loaded graphite epoxy panels with square and elliptical cut-outs", *Thin-Wall. Struct.*, **28**(3), 373-397.

Biswal, M., Sahu, S., Asha, A. and Nanda, N. (2016), "Hygrothermal effects on buckling of composite shell-experimental and FEM results", *Steel Compos. Struct., Int. J.*, **22**(6), 1445-1463.

Bohlooly, M. and Mirzavand, B. (2015), "Closed form solutions

for buckling and postbuckling analysis of imperfect laminated composite plates with piezoelectric actuators", *Compos.*: *Part B*, **72**(1), 21-29.

Bohlooly, M. and Mirzavand, B. (2016), "Thermomechanical buckling of hybrid cross-ply laminated rectangular plates", *Adv. Compos. Mater.*, **65**(11), 1780-1790.

Britt, V. (1993), "Shear and compression buckling analysis for anisotropic panels with centrally located elliptical cutouts", *AIAA*, **32**(11), 2293-2299.

Chen, Q. and Qiao, P. (2014), "Post-buckling analysis of composite plates under combined compression and shear loading using finite strip method", *Finite Elem. Anal. Des.*, **83**(1), 33-42.

Department of Defense United States America (2002), The composite material handbook-MIL 17: polymer matrix composite guidelines for characterization of structure materials; ASTM International, PA, USA.

Desalvo, G, (1983), *ANSYS Engineering Analysis System Verification Manual*, Swanson Analysis System, Houston, KA, USA.

Eladi, F. and Alecakir, S. (2006), "Damage tolerance of stiffened composite panels with cutouts", *J. Reinf. Plast. Compos.*, **25**(13), 1341-1351.

Ghannadpour, S.A.M., Najafi, A. and Mohammadi, B. (2006), "On the buckling behavior of cross-ply laminated composite plates due to circular/elliptical cutouts", *Compos. Struct.*, **75**(3), 3-7.

Hyre, M. and Lee, H. (1991), "The use of curvilinear fiber format to improve buckling resistance of composite plates with central circular holes", *Compos. Struct.*, **18**(3), 239-261.

Jain, P. and Kumar, A. (2004), "Post buckling response of square laminates with a central circular/elliptical cutout", *Compos. Struct.*, **65**(2), 179-185.

Jamali, M., Shojaee, T., Kolahchi, R. and Mohammadi, B. (2016), "Buckling analysis of nanocomposite cut out plate using domain decomposition method and orthogonal polynomials", *Steel Compos. Struct., Int. J.*, **22**(3), 691-712.

Jaunky, N. (2001), "Progressive failure studies of composite panels with and without cutouts", *NASA Langley Res. Center*, VA, USA, September.

Kumar, D. and Singh, S.B. (2010), "Effects of boundary conditions on buckling and post buckling responses of composite laminate with various shaped cutouts", *Compos. Struct.*, **92**(3),769-779.

Kumar, D. and Singh, S.B. (2011), "Load interaction curves and post-buckling response of composite laminate with circular cutout under combined in-plane loading", *Compos.*: *Part B*, **42**(5),1189-1195.

Larsson, P. (1989), "On buckling of orthotropic stretched plates with circular holes", *Compos. Struct.*, **11**(11), 121-134.

Lin, C. and Kuo, C. (1989), "Buckling of Laminated Plates with Holes", *J. Compos. Mater.*, **23**(6), 536-553.

Lopatin, A.V. and Morozov, E.V. (2013), "Buckling of a uniformly compressed rectangular SSCF composite sandwich plate", *Compos. Struct.*, **105**(1), 108-115.

Lu, H., Li, J., Nie, C., Duan, B., Yin, W., Yin, J., Hui, D. and He, X. (2017), "Study on buckling response in electrospun fiber with periodic structure", *Compos.*: *Part B*, **113**(1), 270-277.

Martin, J. (1972), "Buckling and post buckling of laminated composite square plates with reinforced central holes", Ph.D. Dissertation; Case Western Reserve University, Cleveland, OH, USA.

Moen, C. and Schafer, B.W. (2009), "Elastic buckling of thin plates with holes in compression or bending", *Thin-Wall. Struct.*, **47**(12), 1597-1607.

Narayana, A.L., Kumara, R.V. and Rao, G.K. (2018), "Effect of volume fraction on the thermal buckling analysis of laminated composite plate with square/rectangular cutout", *Mater. Today*: *Proceedings of 7th Int. Conf. Materials Processing and Characterization*, **5**(1), 5819-5829.

Nemeth, M. (1988), "Buckling behavior of compression-loaded symmetrically laminated angle-ply plates with holes", *AIAA J.*, **26**(3), 330-336.

Nemeth, M. (1989), "Buckling and post buckling behavior of square compression-loaded graphite-epoxy plates with circular cutouts", *Proceedings of Conference on Fibrous Composites in Structural Design*, VA, USA, November.

Niu, M.Y. (1988), Airframe Structural Design, Lockheed Aeronautical System Company Burbank, CA, USA.

Oterkus, E. Barut, A. and Madenci, A. (2004), "Buckling of composite plates with a reinforced circular cutout subjected to uniform and non-uniform compression", *Structural Dynamics, and Materials Conference*, VA, USA.

Sun, F., Wang, P., Li, W., Fan, H. and Fang, D. (2017), "Effects of circular cutouts on mechanical behaviors of carbon fiber reinforced lattice-core sandwich cylinder", *Compos. Part A*: *Appl. Sci. Manuf.*, **100**(1), 313-323.

Talib, A.R., Ramadhan, A., Rafie, A.S. and Zahari, R. (2013), "Influence of cut-out hole on multi-layer Kevlar-29/epoxy composite laminated plates", *Mater. Des.*, **43**(1), 89-98.

Tercan, M. and Aktaş, M. (2009), "Buckling behavior of 1×1 rib knitting laminated plates with cutouts", *Compos. Struct.*, **89**(2), 245-252.

Umut, T. (2013), "Application of a new extended layerwise approach to thermal buckling load optimization of laminated composite plates", *Steel Compos. Struct., Int. J.*, **14**(3), 283-293.

Upadhyay, A.K. and Shukla, K.K. (2013), "Post-buckling behavior of composite and sandwich skew plates", *Int. J. Non-Linear Mech.*, **55**(1), 120-127.

Wang, V., Feng, C., Zhao, Z., Lu, F. and Yang, J. (2018), "Torsional buckling of graphene platelets (GPLs) reinforced functionally graded cylindrical shell with cutout", *Compos. Struct.*, **197**(1), 72-79.

Yazici, M. (2008), "Influence of cut-out variables on buckling behavior of composite plates", *J. Reinf. Plast. Compos.*, **28**(19), 2325-2339.

CC